Radiology

Right Arcuate Fasciculus Abnormality in Chronic Fatigue Syndrome[1]

Michael M. Zeineh, MD, PhD
James Kang, MD
Scott W. Atlas, MD
Mira M. Raman, MS
Allan L. Reiss, MD
Jane L. Norris, PA
Ian Valencia, BS
Jose G. Montoya, MD

Purpose: To identify whether patients with chronic fatigue syndrome (CFS) have differences in gross brain structure, microscopic structure, or brain perfusion that may explain their symptoms.

Materials and Methods: Fifteen patients with CFS were identified by means of retrospective review with an institutional review board–approved waiver of consent and waiver of authorization. Fourteen age- and sex-matched control subjects provided informed consent in accordance with the institutional review board and HIPAA. All subjects underwent 3.0-T volumetric T1-weighted magnetic resonance (MR) imaging, with two diffusion-tensor imaging (DTI) acquisitions and arterial spin labeling (ASL). Open source software was used to segment supratentorial gray and white matter and cerebrospinal fluid to compare gray and white matter volumes and cortical thickness. DTI data were processed with automated fiber quantification, which was used to compare piecewise fractional anisotropy (FA) along 20 tracks. For the volumetric analysis, a regression was performed to account for differences in age, handedness, and total intracranial volume, and for the DTI, FA was compared piecewise along tracks by using an unpaired t test. The open source software segmentation was used to compare cerebral blood flow as measured with ASL.

Results: In the CFS population, FA was increased in the right arcuate fasciculus (P = .0015), and in right-handers, FA was also increased in the right inferior longitudinal fasciculus (ILF) (P = .0008). In patients with CFS, right anterior arcuate FA increased with disease severity (r = 0.649, P = .026). Bilateral white matter volumes were reduced in CFS (mean ± standard deviation, 467 581 mm^3 ± 47 610 for patients vs 504 864 mm^3 ± 68 126 for control subjects, P = .0026), and cortical thickness increased in both right arcuate end points, the middle temporal (T = 4.25) and precentral (T = 6.47) gyri, and one right ILF end point, the occipital lobe (T = 5.36). ASL showed no significant differences.

Conclusion: Bilateral white matter atrophy is present in CFS. No differences in perfusion were noted. Right hemispheric increased FA may reflect degeneration of crossing fibers or strengthening of short-range fibers. Right anterior arcuate FA may serve as a biomarker for CFS.

©RSNA, 2014

Online supplemental material is available for this article.

Radiology

Chronic fatigue syndrome (CFS) is a debilitating disorder characterized by 6 or more months of persistent or relapsing fatigue without any associated medical or psychiatric disorder (1). The high prevalence of 2–4 per 1000 people in the United States (2,3), combined with the profound disability (4) and poor prognosis (5), motivates urgent scientific investigation. Brain imaging could aid in diagnosis and prognosis. However, structural imaging findings have been inconsistent: Three voxel-based morphometry studies demonstrated gray matter atrophy in differing locations when specified (6–8), while one study in which cerebrospinal fluid was segmented yielded no atrophy (9). Brain perfusion studies have shown inconsistent decreases (10), with a well-controlled study of monozygotic twins showing no differences (11). No technique has provided either a pathophysiological understanding of the disorder or served as a biomarker.

With diffusion-tensor imaging (DTI), the random motion of water is used to demonstrate brain microstructure and has been explored across a variety of neurodegenerative disorders. White matter microstructure may be altered in CFS as a consequence of inflammation (12) or as part of the neurocognitive physiology of fatigue (13), but it has not been investigated to date with DTI.

The purpose of this study was to (a) identify differences in gross brain structure in CFS by using T1-weighted gray and white matter volumetric analysis, (b) detect microstructural abnormalities underlying CFS by using DTI, and (c) detect global alterations in brain perfusion by using pseudocontinuous arterial spin labeling (ASL).

Materials and Methods

Subjects

This study began in June 2011, and follow-up was completed in November 2013. Institutional review board approval with a waiver of consent and a waiver of authorization were obtained, and a retrospective review was conducted from 2008 to the present for patients evaluated in the university CFS clinic. Inclusion criteria were (a) the clinical criteria for CFS (fatigue for a duration of 6 months or longer, along with having at least four of the eight Fukuda symptoms: impaired memory or concentration, sore throat, tender lymph nodes, headaches, muscle pain, joint pain, unrefreshing sleep, and postexertional malaise) and (b) ongoing memory and concentration symptoms that cause a severe enough impairment that the physician determined clinical magnetic resonance (MR) imaging was appropriate to exclude other diagnoses. All patients with CFS except one were evaluated by one clinician (J.G.M., with 10 years of experience with CFS). No other inclusion or exclusion criteria were used for patients with CFS. Among 259 charts reviewed, 15 patients were identified who met these criteria, and

none of these patients were excluded. More than 300 control subjects from a database of volunteers were examined to find age-matched (within 1 year) and sex-matched participants without any history of major depression, CFS or chronic fatigue, or substance abuse in the past year; 28 eligible volunteers were contacted, and 14 chose to participate and underwent MR imaging. Control subjects provided informed consent in accordance with the institutional review board and the Health Insurance Portability and Accountability Act. The 20-item Multidimensional Fatigue Inventory (MFI-20) was administered to each subject, which has been validated as a reproducible instrument for the identification of CFS (14–17). The MFI-20 score is used to assess general, physical, and mental fatigue, as well as reduced motivation and activity; higher MFI-20 scores indicate increased severity. Subjects completed an expanded Edinburgh handedness inventory (http://www.brainmapping.org/shared/Edinburgh.php), with scores thresholded at 48

Advances in Knowledge

- Patients with severe chronic fatigue syndrome (CFS) have increased fractional anisotropy (FA) in the anterior right arcuate fasciculus when compared with control subjects ($P = .0015$), with most right-handed patients having maximal FA in the anterior 10% of the arcuate of higher than 0.6, while in the same region, most right-handed control subjects have an FA of less than 0.6.

- The right hemisphere in younger patients with CFS exhibits regions of cortical thickening that are connected via the right arcuate fasciculus, specifically in the right middle temporal and precentral gyri.

- White matter volumes are lower in patients with CFS compared with control subjects (467 581 mm^3 ± 47 610 vs 504 864 mm^3 ± 68 126, $P = .0026$).

Implication for Patient Care

- Right anterior arcuate FA may be a biomarker for CFS.

Author contributions:
Guarantors of integrity of entire study, M.M.Z., J.K., J.G.M.; study concepts/study design or data acquisition or data analysis/interpretation, all authors; manuscript drafting or manuscript revision for important intellectual content, all authors; approval of final version of submitted manuscript, all authors; agrees to ensure any questions related to the work are appropriately resolved, all authors; literature research, M.M.Z., J.K., J.G.M.; clinical studies, M.M.Z., J.K., S.W.A., J.L.N., I.V., J.G.M.; experimental studies, M.M.Z., J.K., A.L.R., I.V.; statistical analysis, M.M.Z., J.K., A.L.R.; and manuscript editing, M.M.Z., J.K., S.W.A., A.L.R., I.V., J.G.M.

and higher. Four subjects declined this inventory and simply described themselves as left-handed, right-handed, or ambidextrous. Left-handed and ambidextrous subjects were pooled as non–right-handed subjects.

MR Imaging Acquisition

Subjects were imaged with one of two identical GE 3T 750HDx 60-cm–bore magnets (with scheduling dictating the imaging unit chosen) by using an eight-channel phased-array receive-only head coil and body-transmit coil. For volumetric assessment, we performed axial three-dimensional T1-weighted inversion-recovery spoiled gradient-echo and three-dimensional axial brain volume imaging with array spatial sensitivity encoding technique acceleration of 2, or ASSET 2, (repetition time msec/echo time msec, 9.15/3.7; inversion time msec, 450; flip angle, 13°; bandwidth, 25; field of view, 240 mm; 256 × 256 matrix; 1.2-mm-thick sections; 130 sections acquired; imaging time, 2 minutes 50 seconds). Two diffusion-weighted sequences were performed, the first with higher spatial resolution and the second with higher angular resolution: *(a)* one b of 0 mm/sec^2 image acquired, 40 directions at b of 2000 mm/sec^2, twice refocused, two-dimensional axial, ASSET 2, frequency right/left, 8000/95.5, field of view of 240 mm, 128 × 128 matrix reconstructed at 256 × 256, 2-mm-thick sections with 0-mm gap, 59 sections acquired, two signals acquired, and imaging time of 11 minutes; *(b)* and one b of 0 mm/sec^2 image acquired, 50 directions at b of 2000 mm/sec^2, twice-refocused two-dimensional axial, ASSET 2, frequency right/left, 8000/90.2, field of view of 240 mm, 96 × 96 matrix reconstructed at 256 × 256, 4-mm-thick sections with 0-mm gap, 36 sections acquired, two signals acquired, and imaging time of 13 minutes 44 seconds. Pseudocontinuous ASL was performed (three-dimensional axial imaging, 4800/10.6, bandwidth of 62, field of view of 220, 128 × 128 matrix, 4-mm-thick sections, 63 sections acquired, three signals acquired with one signal acquired for the unlabeled proton-density image, and imaging time of 4 minutes 50 seconds). One patient with CFS did not undergo ASL imaging because of a technical error.

Segmentation: Volumetry

A FreeSurfer pipeline analysis conducted by using the T1-weighted images *(http://surfer.nmr.mgh.harvard.edu/)* produced cortical, white matter, and subcortical segmentations (18). These segmentations underwent blinded manual editing (by J.K., with 2 years of neuroradiology experience, and M.M.Z., with 17 years of segmentation and quantitative neuroimaging experience) to improve skull stripping (typically, portions of the skull base, dura, and dural venous sinuses are erroneously characterized as cortex), extend the white matter segmentation to include all subcortical white matter (due to residual B0 inhomogeneity after correction), and retract the white matter segmentation when it seeps into the cortex (which occurs near primary somatosensory cortex at the vertex with its inherently reduced contrast with the subjacent white matter at T1-weighted imaging) (19). An additional step of blinded manual editing was performed for quantification of subcortical gray structures by using FreeView (by removing extra voxels from the hippocampal and thalamic segmentations). This produces a complete segmentation of the cortex, supratentorial white matter, deep gray nuclei, and ventricles. For computing total intracranial volume, we summed the supratentorial gray matter, supratentorial white matter, and cerebrospinal fluid compartments (the latter was estimated from the sulcal, lateral, and third ventricular and choroid plexus volumes).

DTI Acquisition

The DTI acquisitions were imported separately, along with the T1-weighted volume, into two separate and independent instances of automated fiber quantification *(http://white.stanford.edu/newlm/index.php/AFQ,* performed by M.M.Z.) (20). Imaging volumes were inspected manually, and occasional artifactual diffusion-weighted imaging volumes were excluded from analysis. Data were corrected for motion with a rigid-body transformation and aligned to the b of 0 mm/sec^2 image, which was then aligned to the T1-weighted volume in anterior commissure–posterior commissure space. Automated fiber quantification performs automated tractography of 20 tracks, nine in each hemisphere (anterior thalamic radiations, corticospinal, cingulate cingulum, parahippocampal cingulum, inferior frontal occipital fasciculus, inferior longitudinal fasciculus [ILF], superior longitudinal fasciculus, uncinate fasciculus, and arcuate fasciculus) and two bilateral tracks (forceps major and minor of the corpus callosum). Each tract *(a)* was cleaned of extraneous fibers that deviated too far from the fiber core and truncated at standard region-of-interest (ROI) positions and *(b)* was normalized to 100 pixels in length. With this process, some tracks could be identified in all subjects.

ASL Acquisition

ASL signal intensity was divided by signal intensity in coplanar proton-density images and multiplied by a scaling factor to deliver maps of cerebral blood flow in milligrams per milliliter per minute (21) *(www.nmr.mgh.harvard.edu/~jjchen/ASL.html)*. The proton-density image acquired as part of the ASL sequence was used to align with the T1-weighted volume by using the FMRIB (Functional MRI of the Brain) Software Library, or FSL, "flirt" function with six degrees of freedom and a normalized mutual information cost function, so cerebral blood flow images were in the same space as the FreeSurfer segmentations. This alignment was manually inspected by M.M.Z. to ensure accuracy. Cerebral blood flow was averaged over the segmentations of the cerebral cortex, supratentorial white matter, basal ganglia, thalamus, and hippocampi.

Statistical Analysis

All statistical analyses were performed by M.M.Z. For all volumetric comparisons, a regression was computed by using age, total intracranial volume,

disease, and handedness as independent variables, a recommended procedure for these types of analyses (22), by using Stata software (StataCorp, College Station, Tex). Uncorrected *P* values for the comparison of the volumes of the six regions evaluated—cortical gray matter, supratentorial white matter, thalami, hippocampi, basal ganglia, and rostral middle frontal gyri—are reported, along with the Bonferroni-corrected threshold for significance (.05/6 = .0083). The right and left white matter compartments and middle frontal gyri were evaluated separately by using the same regression procedure. Exclusively within the CFS population, a Pearson correlation coefficient was computed between regional volumes and MFI-20 scores.

For the cortical thickness evaluation, we first made global comparisons by examining the mean cortical thickness across both hemispheres together, again comparing via regression. We then used the FreeSurfer "qdec" module to compare cortical thickness between the CFS group and the control group, regressing age as a covariate (22), and handedness as an additional discrete factor. By using a different offset and different slope for each group and smoothing of 10 mm, we corrected for multiple comparisons with a false-discovery rate of .05. Cortical thickness was regressed in the CFS group with MFI-20 scores as an additional covariate, also by using "qdec."

For the DTI, fractional anisotropy (FA) was sampled along each identified track and compared piecewise between groups by using an unpaired *t* test to compare both cohorts. Additional testing was performed in right-handed individuals from each group because differences in language lateralization can affect several tracks (including the right arcuate) (23). Automated fiber quantification uses a permutation-based method to correct for multiple comparisons between groups along a single track (24), producing a threshold *P* value equivalent to a corrected *P* value of .05. These *P* value thresholds vary per track, likely because tracks have unique correlation structures

based on regional differences in subject anatomy, as well as differences attributable to crossing fibers. A track had a significant difference if the *P* value for the *t* test was below this threshold for at least one point along the track. The high-spatial-resolution first DTI acquisition was used to generate a hypothesis: All tracks were tested for significant differences of FA, correcting for multiple comparisons within each track, but not across all tracks. The high-angular-resolution second DTI acquisition was used to test a hypothesis: Significant results from the hypothesis-generating data set were tested individually for significant differences in FA, correcting for multiple comparisons within each track, and not needing a correction across tracks because of the focused hypothesis testing. Maximal FA and mean axial diffusivity and radial diffusivity were computed over the anterior 10% of the right arcuate fasciculus. This maximal FA was correlated with the subject's MFI-20 scores separately for patients and control subjects. Axial diffusivity and radial diffusivity were compared between groups by using an unpaired *t* test. A receiver operating characteristic (ROC) curve was plotted separately for the hypothesis-generating and hypothesis-testing data sets by identifying the accuracy of using maximal FA in the anterior 10% of the right arcuate fasciculus to diagnose CFS across multiple FA thresholds (with the FA threshold spaced .05 apart) by using Excel (Microsoft, Redmond, Wash). The 95% confidence intervals (CIs) for sensitivity and specificity were computed by using the Stata "diagti" module, and the area under the ROC curve was determined with the function "roctab." For combined visualization of tractography and cortical thickness results, we first depicted the right arcuate and right ILF in one subject by using automated fiber quantification. Then, we drew ROIs around the three largest clusters of significantly different thicknesses by using "qdec" and transformed the ROIs into this single subject's native space. To plot these ROIs alongside the tractography, the center of mass for each cluster was extracted by using FSL

"fslstats" (25,26), and a spheroid was plotted with a volume equal to the cluster volume by using MATLAB software (Mathworks, Natick, Mass).

For the ASL, unpaired *t* tests were used to compare cerebral blood flow for each of the regions between groups, with *P* values reported uncorrected.

The results of all automated steps were verified by M.M.Z. either visually or numerically for plausibility. All results were interpreted with agreement by M.M.Z., A.L.R, M.M.R, J.K., and J.G.M.

Results

Clinical Data

Thirteen of the 15 patients with CFS and 10 of 14 control subjects were right-handed. Women constituted 55% of participants (eight patients with CFS and eight control subjects), and 45% of the participants were men (seven patients with CFS and six control subjects). Mean age ± standard deviation was 46.2 years ± 14.2 (range, 20–66 years) and was statistically equivalent for women and men (46.6 years ± 15.6 [range, 20–66 years] for women vs 45.6 years ± 12.9 [range, 23–60 years] for men; *P* = .86). Mean ages of the CFS and control groups were statistically equivalent (46.5 years ± 13.2 and 46.6 years ± 14.6, respectively; *P* = .98). MFI-20 scores were significantly different from patients compared with control subjects (MFI-20: 79.60 years ± 15.3 vs 27.64 years ± 8.54, respectively; *P* < .001). The mean duration of symptoms for CFS participants was 12.1 years ± 6.9.

Segmentation

Volumetry.—For the entire cohort, there was significantly lower total supratentorial white matter volume for patients with CFS compared with control subjects, when accounting for age, total intracranial volume, and handedness (Table 1). This reduction was present bilaterally (left, *P* = .0035; right, *P* = .0033). Additionally, total thalamic volume tended to be lower in CFS, but this did not reach significance after

Table 1

Volumetry Comparison between Patients with CFS and Control Subjects and Correlation with MFI-20 Score

Brain Region	Volume in Patients with CFS (mm³)	Volume in Control Subjects (mm³)	β Value for the Fitted Slope	P Value for Disease Status in Regression Analysis	r Value for MFI-20 Scores in CFS	Bonferroni-corrected P Values
Cortical gray matter	448 899 ± 59 082	449 627 ± 47 163	13 120	.0728	0.3658	.1800
Supratentorial white matter	467 581 ± 47 610*	504 864 ± 68 126*	−17 439*	.0026*	0.0214	.9396
Thalami	13 115 ± 1870	14 430 ± 1812	−1009	.0469	0.2196	.4317
Hippocampi	7655 ± 528	7950 ± 781	−284	.1341	0.1256	.6555
Basal ganglia	18 982 ± 2951	19 321 ± 2832	72	.8934	0.5564	.0312
Rostral middle frontal gyri	30 323 ± 5471	30 144 ± 4733	1711	.1357	0.2343	.4006

Note.—r values demonstrate the correlations between CFS patient volumes and their corresponding MFI-20 scores. r values were calculated with the Pearson correlation coefficient and are shown with the associated P values, with a Bonferroni-corrected threshold of .0083 (to control for the six regions tested).

* Significant difference.

correction for multiple comparisons. Total cortical gray matter volume was statistically equivalent. Prefrontal cortex volumes (identified in other studies of CFS, where foci are best matched by the rostral middle frontal gyri as segmented with FreeSurfer) (6,27) were also statistically equivalent between groups. However, the right middle frontal gyrus trended toward increased volume in the CFS group (15 446 mm³ ± 2771 in the CFS group and 14 721 mm³ ± 2158 in control subjects; $P = .0212$). Within the CFS population, the MFI-20 score trended toward a positive correlation with basal ganglia volume ($r = 0.5564$, $P = .0312$).

Thickness.—Global cortical thickness was equivalent between populations (2.437 mm ± 0.102 in patients with CFS vs 2.418 mm ± 0.091 in control subjects; $P = .932$) (Table 2, Fig 1). No focal left hemispheric differences were present. However, the right hemisphere demonstrated five regions of increased cortical thickness when accounting for age and handedness, which was most notable in the younger, not the older, patients with CFS, with no regions of decreased cortical thickness (Table 2, Fig 1). No regions demonstrated cortical thickness that increased significantly with age. No significant correlations with MFI-20 were present bilaterally in the CFS group.

DTI in all subjects, right- and left-handed.—In the high-resolution hypothesis-generating data set, the

Table 2

Regions of Significant Increases in Right-Hemispheric Cortical Thickness in Patients with CFS Compared with Control Subjects, Corrected for Multiple Comparisons

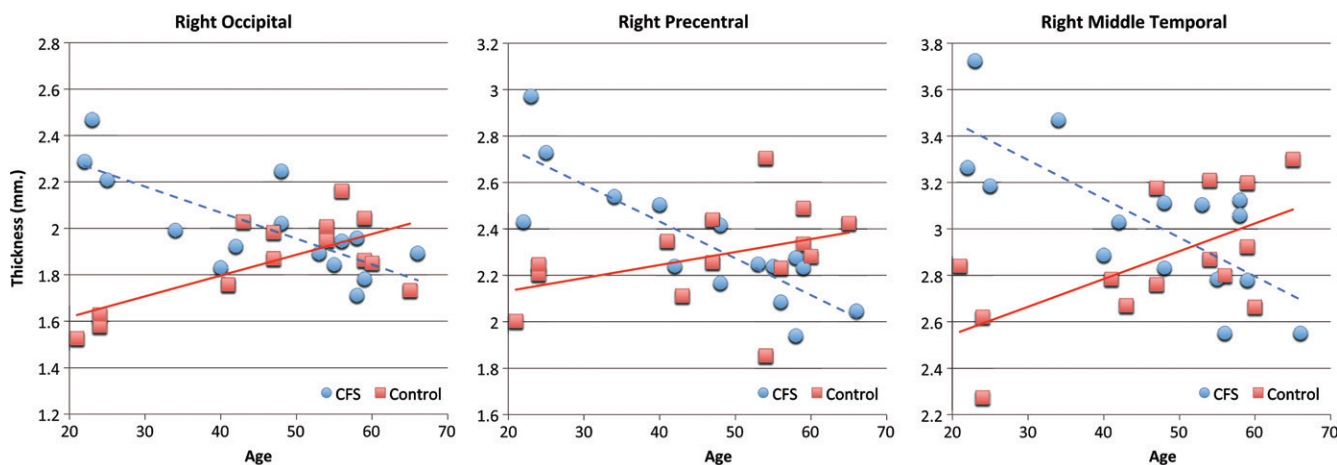| Location	Area (mm²)	T Score	X Value	Y Value	Z Value
Lateral occipital	100.14	5.3592	25.3	−88.4	−9
Precentral	89.19	5.3675	40.4	−10.7	34
Middle temporal	35.84	4.2466	63.3	−25.5	−12.3
Postcentral	16.84	4.5786	61.4	−11.9	17.2
Pars orbitalis	8.83	4.0795	40.2	48.4	−4.9

Note.—X, Y, and Z refer to Montreal Neurological Institute 305 coordinates.

only significant difference was that the anterior right arcuate fasciculus (identified in 13 of 15 patients and 14 of 14 control subjects) demonstrated significantly higher FA in patients compared with control subjects, correcting for multiple-comparisons within but not across tracks (Table 3; Figs 2, 3). By performing the same unpaired t test just on the right arcuate fasciculus in the second hypothesis-testing DTI data set (also identified in 13 of 15 patients and 14 of 14 control subjects), we confirmed with a highly significant P value the same result by testing this single hypothesis ($P = .0001$, significant after correction within track). This FA increase was accompanied by an increase in axial diffusivity ([1.117 ± 0.089] × 10⁻³ mm²/sec for patients with CFS vs [1.005 ± 0.084] × 10⁻³ mm²/sec for control subjects, averaged over the anterior 10% of the arcuate
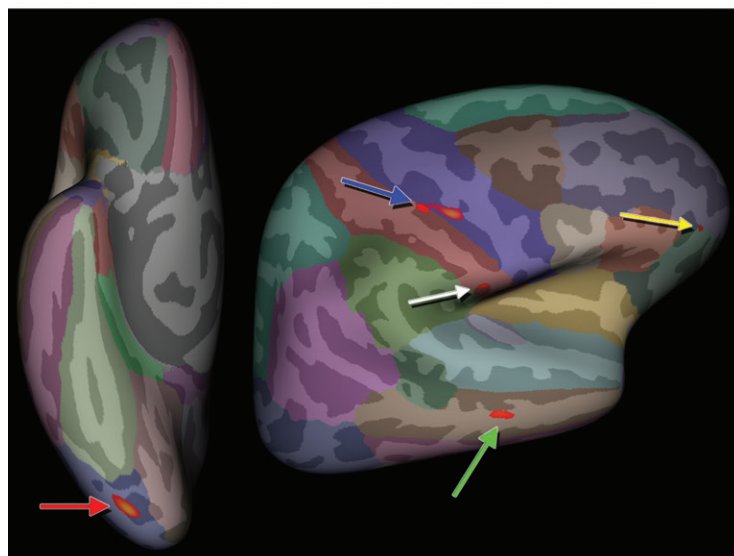
fasciculus, pixel positions 90–100) and a decrease in radial diffusivity (0.364 ± 0.069 for patients vs 0.425 ± 0.039 for control subjects). The correlation between maximal FA over the same portions of this track and MFI-20 in the CFS population was not significant ($r = 0.276$, $P = .4$). Of note, the two end points of the right arcuate fasciculus are adjacent to the region of increased cortical thickening in the right precentral and middle temporal gyri (Figs 1, 3; Movie 1 [online]).

DTI in right-handed subjects only.—Right anterior arcuate FA was again significantly increased in CFS (Fig 2a, first DTI acquisition, $P = .0006$; Fig 2b, second DTI acquisition, $P = .00036$; both highly significant after correction within track). The correlation between maximal FA over the anterior 10% of this track and MFI-20 in the CFS population was significant in

Figure 1

a.

b.

Figure 1: **(a)** Plots of cortical thickness are shown according to age in the right occipital, precentral, and middle temporal gyral ROIs. **(b)** Superimposed on the inflated atlas brain image are regions of right-hemisphere increased cortical thickness in patients with CFS compared with control subjects after accounting for differences in age and handedness are highlighted in red (arrows). Blue = precentral, green = middle temporal, red = occipital, white = postcentral, and yellow = orbitofrontal. The right precentral region consists of two connected foci that FreeSurfer identified as one contiguous region.

the hypothesis-generating data set but not the hypothesis-testing data set ($r = 0.649$ [$P = .026$] and $r = 0.472$ [$P = .136$], respectively). There was no correlation between MFI-20 and the same pixel locations in control subjects ($r = -0.02$). FA was also increased in the right anterior ILF (Figs 2c, 2d, 3; first DTI acquisition, $P = .0008$; second DTI acquisition, $P = .0018$; both significant after correcting within track). However, the peak FA was of greater magnitude difference and more consistent in location in the arcuate fasciculus compared with the ILF. The occipital lobe end point of the ILF was adjacent to the

right occipital region of cortical thickening (Figs 1, 3; Movie 1 [online]).

An ROC curve was calculated by using maximal FA in the anterior 10% of the right arcuate fasciculus to diagnose CFS in right-handed patients (Fig 4 shows the hypothesis-testing data set ROC). A threshold of 0.6 would be used to correctly diagnose CFS in right-handed patients in the hypothesis-generating data set, with a sensitivity, specificity, and area under the ROC curve of 81.8% (95% CI: 48.2%, 97.7%), 100% (95% CI: 69.2%, 100%), and 0.918 (95% CI: 0.696, 0.988), respectively. In the

hypothesis-testing data set, the same measurements were 72.7% (95% CI: 39.0%, 94.0%), 90.0% (95% CI: 55.5%, 99.7%), and 0.891 (95% CI: 0.696, 0.98) respectively.

ASL Findings

ASL demonstrated no significant difference in perfusion to the cortex (672 mL per 100 mg per minute ± 123 for patients with CFS vs 633 mL per 100 mg per minute ± 145 for control subjects; $P = .39$), supratentorial white matter (495 mL per 100 mg per minute ± 88 for patients with CFS vs 496 mL per 100 mg per minute ± 113 for control subjects; $P = .84$), basal ganglia (523 mL per 100 mg per minute ± 84 for patients with CFS vs 512 mL per 100 mg per minute ± 081 for control subjects; $P = .69$), thalami (599 mL per 100 mg per minute ± 116 for patients with CFS vs 587 mL per 100 mg per minute ± 116 for control subjects; $P = .78$), or hippocampi (587 mL per 100 mg per minute ± 106 for patients with CFS vs

Table 3

Statistical Tests for Significance of Difference in FA across Tracks

Track	All Patients			Right-Handers		
	P Value	P Value Threshold	No. of Patients and Control Subjects with Track Present	P Value	P Value Threshold	No. of Patients and Control Subjects with Track Present
Left thalamic radiation	.2144	.0027	15, 14	.0891	.0022	13, 10
Right thalamic radiation	.0360	.0019	15, 14	.0585	.0031	13, 10
Left corticospinal	.0087	.0033	15, 14	.0050	.0026	13, 10
Right corticospinal	.0499	.0024	15, 14	.0620	.0034	13, 10
Left cingulum cingulate	.0029	.0012	15, 14	.0054	.0013	12, 10
Right cingulum cingulate	.1325	.0019	15, 14	.2324	.0016	13, 10
Left cingulum hippocampus	.0566	.0021	15, 14	.0979	.0023	13, 10
Right cingulum hippocampus	.1107	.0027	14, 14	.0483	.0023	12, 10
Callosum forceps major	.0854	.0016	13, 14	.0603	.0011	13, 10
Callosum forceps minor	.1175	.0022	15, 14	.1404	.0022	13, 10
Left inferior fronto-occipital fasciculus	.0133	.0014	15, 14	.0383	.0013	13, 10
Right inferior fronto-occipital fasciculus	.0099	.0011	15, 14	.0285	.0015	11, 10
Left ILF	.0041	.0026	15, 14	.0149	.0019	13, 10
Right ILF	.0055	.0022	14, 14	.0008*	.0015	13, 10
Left superior longitudinal fasciculus	.0842	.0040	15, 14	.0861	.0045	13, 10
Right superior longitudinal fasciculus	.1001	.0045	15, 14	.0873	.0046	13, 10
Left uncinate	.2574	.0031	15, 14	.0622	.0025	13, 10
Right uncinate	.2390	.0051	15, 14	.0606	.0034	13, 10
Left arcuate	.0210	.0022	15, 14	.0343	.0016	13, 10
Right arcuate	.0015*	.0023	13, 14	.0006*	.0028	11, 10

* P values are significant after correcting for multiple comparisons within the track (ie, under the P value threshold).

mL per 100 mg per minute ± 118 for control subjects; $P = .84$).

Discussion

This DTI study of CFS demonstrated increased FA in the right anterior arcuate fasciculus, and this increase correlated with disease severity. An automated, user-independent, microstructural DTI analysis identified this increased FA and verified it in a second data set from the same subjects analyzed independently. In right-handed patients with CFS, this increase was correlated with the patients' MFI-20 scores. Thus, in populations of CFS that have severe concentration and memory problems, right anterior arcuate FA may serve as a biomarker for the disease. An analysis of volumetric data in the same subjects was used to identify reduced bilateral supratentorial white matter volumes, suggesting a global white matter process.

Additionally, two cortical regions connected via the arcuate fasciculus exhibited increased thickness (28–30): the right middle temporal and precentral gyri. Similarly, in right-handers, the ILF showed that increased FA anteriorly increased thickness of a corresponding right occipital region. Our examination yielded no differences in perfusion.

While microstructure has not been studied to date in CFS, increased FA is an unexpected finding for a disorder characterized by reduced cognitive abilities. However, increased FA has been previously reported in the corona radiata in Alzheimer disease (31), possibly due to degeneration of crossing fibers. Given that the difference in CFS only involved the anterior 10% of the arcuate, we suspect this local phenomenon could represent strengthening of fibers that join a small portion of the anterior arcuate, or alternatively a weakening

of crossing fibers. Consistent with our study, others have reported that the right arcuate fasciculus is sometimes not found with tractography, in part because the arcuate is more lateralized to the left hemisphere in right-handers (23,32). We found that arcuate differences between patients with CFS and control subjects were most striking among right-handed patients, suggesting that hemispheric differences with handedness and language (23) are an additional source of variance.

Our volumetry results stand in contradistinction to the literature and show reduced gray matter volumes, either globally or in the prefrontal cortices (6,7,27,33). In fact, we found that the prefrontal volumes trended toward being slightly higher in patients with CFS. Previous investigators have exclusively used voxel-based morphometry, which is based on many factors other than cortical
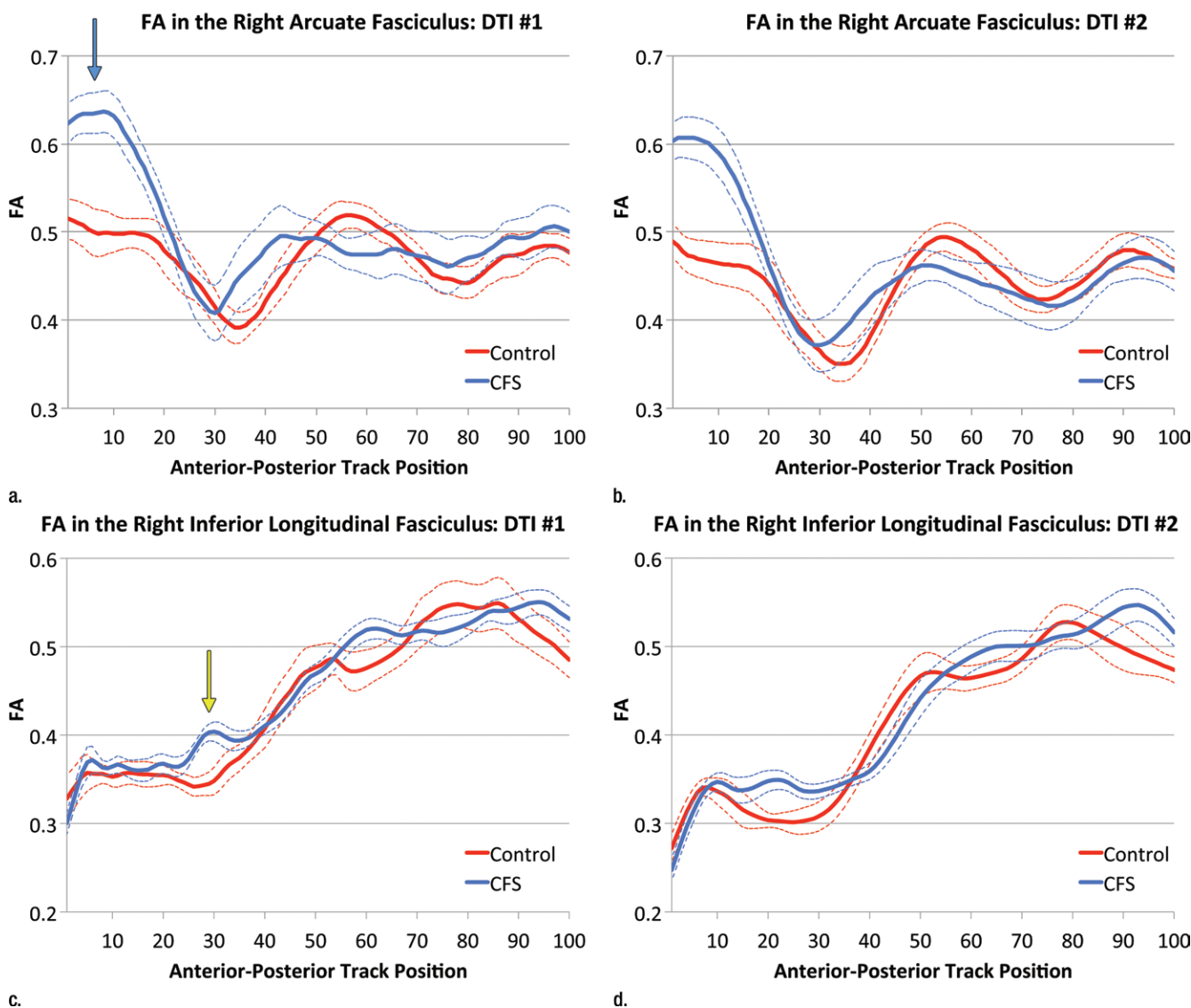
Figure 2

Figure 2: **(a)** FA is plotted along the right arcuate fasciculus from the first diffusion-weighted acquisition; anterior = 0, posterior = 100. Thin blue dotted lines correspond to ±1 standard error. Only right-handers are included in this Figure. The blue arrow highlights the region of maximal increase of FA in patients with CFS compared with control subjects. **(b)** A plot is given for the second diffusion-weighted acquisition. **(c, d)** Similar plots are given for the right ILF, with the yellow arrow on **c** similarly highlighting the region of maximal increase of FA.

thickness (34). The discordance between the literature and our results may be explained by our precise methods, with a careful examination of cortical architecture and correction for covariates, such as age and total intracranial volume (22).

Although we did not control for caffeine exposure (35), our negative ASL result is consistent with a well-controlled perfusion study of CFS involving monozygotic twins (11), suggesting perfusion is not affected in CFS.

Even though the hypothesis-testing data set confirms the veracity of increased FA in the right anterior arcuate, it was determined in the same subjects and cannot be considered a fully independent data set. The correlation between MFI-20 and right anterior arcuate FA was only significant in the hypothesis-generating data set, not the hypothesis-testing data set. Although this may be technically related to the reduced spatial resolution of the latter data set, the utility of arcuate FA as a disease biomarker cannot be conclusively confirmed on this study. While the regions of increased cortical
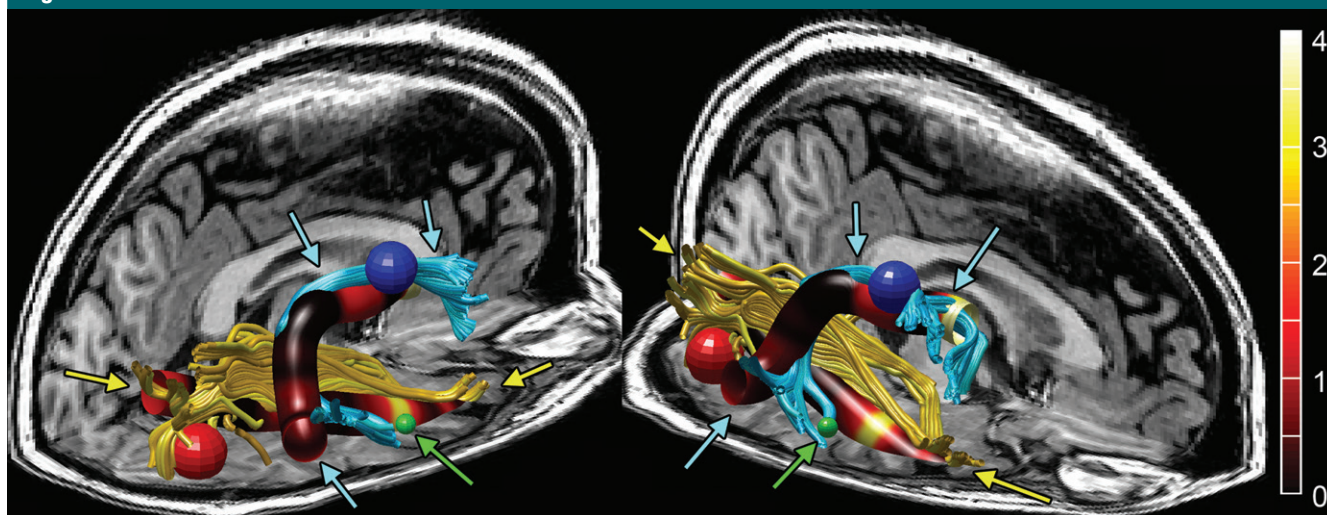
Figure 3: Reconstructed MR image shows the right arcuate (blue tracks and arrows) and ILFs (yellow tracks and arrows) in a single representative subject. These two tracks are overlaid on their respective track profiles (the centroid of each track was averaged across subjects and depicted as the large tubular structures at the core of each track). The track profile is colored according to the *T* score of track-based FA, showing that the maximal increase in FA is in the anterior arcuate and ILFs. The red, blue, and green spheres correspond to size and locations of increased cortical thickness from Figure 1 in the right occipital, precentral, and middle temporal regions, respectively. The green arrows also point to the middle temporal region of increased thickness.
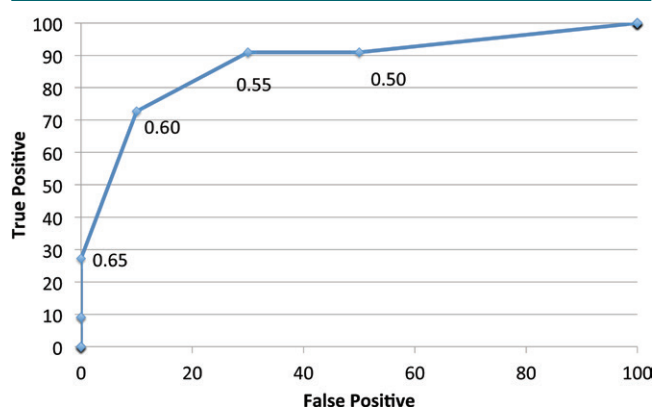

Figure 4: ROC curve is shown for the diagnosis of CFS by measuring the maximal FA in the anterior 10% of the right arcuate fasciculus in right-handers in the hypothesis-testing data set (second DTI acquisition). The number next to each data point indicates the FA threshold for that point in the ROC curve.

thickness are in close proximity to the end points of the arcuate and ILF, these foci are relatively small and imperfectly aligned, suggesting a small effect size. Overall, this study has a small number of subjects, so all of the findings in this study require replication and exploration in a larger group of subjects.

Future work includes validating this finding in a larger right-handed cohort, teasing apart the components of crossing and short-range fibers in the anterior arcuate by using a multiple-shell (multiple *b* value) acquisition and examining the time-course in a longitudinal study, possibly with interventions, and investigating right-hemisphere networks with resting-state functional MR imaging.

References

1. Fukuda K, Straus SE, Hickie I, Sharpe MC, Dobbins JG, Komaroff A. The chronic fatigue syndrome: a comprehensive approach to its definition and study. International Chronic Fatigue Syndrome Study Group. Ann Intern Med 1994;121(12): 953–959.

2. Reyes M, Nisenbaum R, Hoaglin DC, et al. Prevalence and incidence of chronic fatigue syndrome in Wichita, Kansas. Arch Intern Med 2003;163(13):1530–1536.

3. Jason LA, Richman JA, Rademaker AW, et al. A community-based study of chronic

fatigue syndrome. Arch Intern Med 1999;159(18):2129–2137.

4. Natelson BH, Johnson SK, DeLuca J, et al. Reducing heterogeneity in chronic fatigue syndrome: a comparison with depression and multiple sclerosis. Clin Infect Dis 1995;21(5):1204–1210.

5. Cairns R, Hotopf M. A systematic review describing the prognosis of chronic fatigue syndrome. Occup Med (Lond) 2005;55(1):20–31.

6. Okada T, Tanaka M, Kuratsune H, Watanabe Y, Sadato N. Mechanisms underlying fatigue: a voxel-based morphometric study of chronic fatigue syndrome. BMC Neurol 2004;4(1):14.

7. de Lange FP, Kalkman JS, Bleijenberg G, Hagoort P, van der Meer JW, Toni I. Gray matter volume reduction in the chronic fatigue syndrome. Neuroimage 2005;26(3):777–781.

8. Puri BK, Jakeman PM, Agour M, et al. Regional grey and white matter volumetric changes in myalgic encephalomyelitis (chronic fatigue syndrome): a voxel-based morphometry 3 T MRI study. Br J Radiol 2012;85(1015):e270–e273.

9. Perrin R, Embleton K, Pentreath VW, Jackson A. Longitudinal MRI shows no cerebral abnormality in chronic fatigue syndrome. Br J Radiol 2010;83(989):419–423.

10. Biswal B, Kunwar P, Natelson BH. Cerebral blood flow is reduced in chronic fatigue syndrome as assessed by arterial spin labeling. J Neurol Sci 2011;301(1-2):9–11.

11. Lewis DH, Mayberg HS, Fischer ME, et al. Monozygotic twins discordant for chronic fatigue syndrome: regional cerebral blood flow SPECT. Radiology 2001;219(3):766–773.

12. Morris G, Maes M. Myalgic encephalomyelitis/chronic fatigue syndrome and encephalomyelitis disseminata/multiple sclerosis show remarkable levels of similarity in phenomenology and neuroimmune characteristics. BMC Med 2013;11:205.

13. Genova HM, Rajagopalan V, Deluca J, et al. Examination of cognitive fatigue in multiple sclerosis using functional magnetic resonance imaging and diffusion tensor imaging. PLoS ONE 2013;8(11):e78811.

14. Smets EM, Garssen B, Bonke B, De Haes JC. The Multidimensional Fatigue Inventory (MFI) psychometric qualities of an instrument to assess fatigue. J Psychosom Res 1995;39(3):315–325.

15. Gentile S, Delarozière JC, Favre F, Sambuc R, San Marco JL. Validation of the French 'multidimensional fatigue inventory' (MFI 20). Eur J Cancer Care (Engl) 2003;12(1):58–64.

16. Reeves WC, Wagner D, Nisenbaum R, et al. Chronic fatigue syndrome—a clinically empirical approach to its definition and study. BMC Med 2005;3:19.

17. Lin JM, Brimmer DJ, Maloney EM, Nyarko E, Belue R, Reeves WC. Further validation of the Multidimensional Fatigue Inventory in a US adult population sample. Popul Health Metr 2009;7:18.

18. Reuter M, Rosas HD, Fischl B. Highly accurate inverse consistent registration: a robust approach. Neuroimage 2010;53(4):1181–1196.

19. Steen RG, Reddick WE, Ogg RJ. More than meets the eye: significant regional heterogeneity in human cortical T1. Magn Reson Imaging 2000;18(4):361–368.

20. Yeatman JD, Dougherty RF, Myall NJ, Wandell BA, Feldman HM. Tract profiles of white matter properties: automating fiber-tract quantification. PLoS ONE 2012;7(11):e49790.

21. Dai W, Garcia D, de Bazelaire C, Alsop DC. Continuous flow-driven inversion for arterial spin labeling using pulsed radio frequency and gradient fields. Magn Reson Med 2008;60(6):1488–1497.

22. Barnes J, Ridgway GR, Bartlett J, et al. Head size, age and gender adjustment in MRI studies: a necessary nuisance? Neuroimage 2010;53(4):1244–1255.

23. Häberling IS, Badzakova-Trajkov G, Corballis MC. Asymmetries of the arcuate fasciculus in monozygotic twins: genetic and nongenetic influences. PLoS ONE 2013;8(1):e52315.

24. Nichols TE, Holmes AP. Nonparametric permutation tests for functional neuroimaging: a primer with examples. Hum Brain Mapp 2002;15(1):1–25.

25. Jenkinson M, Beckmann CF, Behrens TE, Woolrich MW, Smith SM. FSL. Neuroimage 2012;62(2):782–790.

26. Smith SM, Jenkinson M, Woolrich MW, et al. Advances in functional and structural MR image analysis and implementation as FSL. Neuroimage 2004;23(Suppl 1):S208–S219.

27. de Lange FP, Koers A, Kalkman JS, et al. Increase in prefrontal cortical volume following cognitive behavioural therapy in patients with chronic fatigue syndrome. Brain 2008;131(Pt 8):2172–2180.

28. Phillips OR, Clark KA, Woods RP, et al. Topographical relationships between arcuate fasciculus connectivity and cortical thickness. Hum Brain Mapp 2011;32(11):1788–1801.

29. Catani M, Mesulam M. The arcuate fasciculus and the disconnection theme in language and aphasia: history and current state. Cortex 2008;44(8):953–961.

30. Yeatman JD, Dougherty RF, Rykhlevskaia E, et al. Anatomical properties of the arcuate fasciculus predict phonological and reading skills in children. J Cogn Neurosci 2011;23(11):3304–3317.

31. Douaud G, Jbabdi S, Behrens TE, et al. DTI measures in crossing-fibre areas: increased diffusion anisotropy reveals early white matter alteration in MCI and mild Alzheimer's disease. Neuroimage 2011;55(3):880–890.

32. Catani M, Allin MP, Husain M, et al. Symmetries in human brain language pathways correlate with verbal recall. Proc Natl Acad Sci U S A 2007;104(43):17163–17168.

33. Puri BK, Counsell SJ, Zaman R, et al. Relative increase in choline in the occipital cortex in chronic fatigue syndrome. Acta Psychiatr Scand 2002;106(3):224–226.

34. Hutton C, Draganski B, Ashburner J, Weiskopf N. A comparison between voxel-based cortical thickness and voxel-based morphometry in normal aging. Neuroimage 2009;48(2):371–380.

35. Wang DJ, Chen Y, Fernández-Seara MA, Detre JA. Potentials and challenges for arterial spin labeling in pharmacological magnetic resonance imaging. J Pharmacol Exp Ther 2011;337(2):359–366.